JOURNAL OF GEOPHYSICAL RESEARCH, VOL. 102, NO. A7, PAGES 14,049-14,063, JULY 1, 1997

The Wind magnetic cloud and events of October 18 - 20, 1995: Interplanetary properties and as triggers for geomagnetic activity

R. P. Lepping,[1] L. F. Burlaga,[1] A. Szabo,[1] K. W. Ogilvie,[1] W. H. Mish,[1] D. Vassiliadis,[1] A. J. Lazarus,[2] J. T. Steinberg,[2] C. J. Farrugia,[3] L. Janoo,[3] and F. Mariani[4]

Abstract. Late on October 18, 1995, a magnetic cloud arrived at the Wind spacecraft ≈ 175 R_E upstream of the Earth. The cloud had an intense interplanetary magnetic field that varied slowly in direction, from being strongly southward to strongly northward during its ≈ 30 hours duration, and a low proton temperature throughout. From a linear force free field model the cloud was shown to have a flux rope magnetic field line geometry, an estimated diameter of about 0.27 AU, and an axis that was aligned with the Y axis(GSE) within about 25°. A corotating stream, in which large amplitude Alfven waves of about 0.5 hour period were observed, was overtaking the cloud and intensifying the fields in the rear of the cloud. The prolonged southward magnetic field observed in the early part of the cloud produced a geomagnetic storm of $Kp = 7^-$ and considerable auroral activity late on October 18. About 8 hours in front of the cloud an interplanetary shock occurred. About three-fourths the way into the cloud another apparent interplanetary shock was observed. It had an unusual propagation direction, differing by only 21° from alignment with the cloud axis. It may have been the result of the interaction with the postcloud stream, compressing the cloud, or was possibly due to an independent solar event. It is shown that the front and rear boundaries of the cloud and the upstream driven shock had surface normals in good agreement with the cloud axis in the ecliptic plane. The integrated Poynting flux into the magnetosphere, which correlated well with geomagnetic indices, jumped abruptly to a high value upon entry into the magnetic cloud, slowly decreased to zero near its middle, and again reached substantial but sporadic values in the cloud-stream interface region. This report aims to support a variety of ISTP studies ranging from the solar origins of these events to resulting magnetospheric responses.

1. Introduction

This paper presents observations and analyses of a major interplanetary magnetic cloud and surrounding features, including an upstream shock, another "internal" shock-like pulse, and a downstream interaction region, observed in the interval October 18 - 20, 1995 by the Wind spacecraft, which was about 175 R_E upstream of Earth at the time. This is an extension of a preliminary report on this event by *Burlaga et al.* [1996] in which we provide an overall summary of the interplanetary geometrical and physical relationships of the magnetic cloud and its surrounding structures, stressing their intrinsic properties, relevant for future studies of the solar wind-solar connection. We also briefly discuss these properties as possible interplanetary triggers of geomagnetic activity for the support of studies of their influence on the Earth's magnetosphere.

A magnetic cloud is a transient ejection in the solar wind defined by relatively strong magnetic fields, a large and smooth rotation of the magnetic field direction over approximately 0.25 AU at 1 AU, and a low proton β and proton temperature [*Burlaga et al.*, 1981]. Magnetic clouds are ideal objects for solar-terrestrial studies because of their simplicity and their extended intervals of southward and northward magnetic fields [*Burlaga et al.*, 1990]. Approximately 1/3 of the interplanetary manifestations of solar ejecta (also called "CMEs" by some authors) are magnetic clouds [*Gosling*, 1990]. There is an extensive literature on the structure and dynamics of interplanetary magnetic clouds (see the reviews by *Burlaga* [1991; 1995], their solar sources [*Wilson and Hildner*, 1984, 1986; *Rust*, 1994], and their effects on the magnetosheath [*Farrugia and Burlaga*, 1994; *Farrugia et al.*, 1994; *Lepping et al.*, 1996], the magnetosphere [*Lepping et al.*, 1991; *Farrugia et al.*, 1993a, b, c; *Tsurutani et al.*, 1988], and ionosphere [*Freeman et al.*, 1993; *Knipp et al.*, 1993]. A model of the interaction of a magnetic cloud with the magnetosphere and ionosphere has been presented by *Chen et al.* [1995]. The previous studies focused on relatively limited problems, aimed at

[1]Laboratory for Extraterrestrial Physics, NASA Goddard Space Flight Center, Greenbelt, Maryland.
[2]Center for Space Research, Massachusetts Institute of Technology, Cambridge.
[3]Department of the Study of Earth, Oceans,and Space, University of New Hampshire, Durham.
[4]Dipartimento di Fisica, Universita tor Vergata, Roma, Italy.

Paper number 97JA00272.
0148-0227/97/97JA-00272$09.00

understanding various parts of the solar-terrestrial chain of events associated with magnetic clouds. Recent reviews of the association of geomagnetic activity to magnetic clouds and other IMF features are given by *Farrugia et al.* [1997] and *Tsurutani and Gonzalez* [1997].

The Solar-Terrestrial Physics community is now in a unique position to carry out comprehensive studies of the processes connecting solar events, interplanetary structures, and magnetospheric/ionospheric/thermospheric effects. The International Solar Terrestrial Physics (ISTP) Program was designed from the outset to study solar-terrestrial relations using the data acquired from a large armada of scientific spacecraft, including the Global Geospace Science spacecraft (Wind and Polar), the Japanese spacecraft Geotail, five geosynchronous spacecraft from the Department of Defense and National Oceanic and Atmospheric Administration, the IMP 8 spacecraft, and the recently launched European Space Agency spacecraft SOHO, as well as ground-based observations and theoretical investigations. Special efforts to facilitate the communication of the observations and results via the Internet (including via the World Wide Web) have been made by the ISTP Central Data Handling Facility (CDHF) and the Science Planning and Operations Facility (SPOF) [*Mish et al.*, 1995] of the GGS Project in cooperation with the National Space Science Data Center (NSSDC). The coordination of specific scientific investigations focusing on several campaigns is organized by the Inter-Agency Consultative Group (IACG). It is expected that the First IACG Science Campaign will provide a model for the extensive collaborative efforts that are needed to understand solar-terrestrial processes.

Interval 1 of the First IACG Science Campaign is October 18 - 21, 1995, which fortuitously encompasses the October 1995 magnetic cloud and related events observed by Wind. One aim of this paper is to identify the principal interplanetary features of this magnetic cloud that are needed for future studies of the solar causes and the magnetospheric, ionospheric and thermospheric effects of this and similar magnetic clouds. We will briefly discuss a linkage to the magnetosphere with these interplanetary features, but a more comprehensive study of their geomagnetic effects can be found in the work of *Farrugia et al.* [1996]. Also, see *Smith et al.* [1997] for an identification, discussion, and analysis of a candidate solar source for the October magnetic cloud events.

2. Solar Wind Observations

2.1. Overview of Magnetic Field and Plasma Observations

A plot of the magnetic field data [*Lepping et al.*, 1995] and solar wind parameters [*Ogilvie et al.*, 1995] from October 18 (calendar day 291) through October 20 is shown in Figure 1; all data are 1 min averages. From top to bottom, Figure 1 shows the magnetic field strength (B), the elevation (θ) and azimuth (ϕ) angles of the magnetic field direction in GSE coordinates, the proton number density (N), the most probable proton thermal speed assuming an isotropic Maxwellian velocity distribution ($V_T = \sqrt{(2\ kT/m)}$), and the magnitude of the bulk velocity (V). The magnetic cloud is the region in which the direction of the strong magnetic field rotated more or less smoothly from south to north. The cloud's average speed was ≈ 405 km/s, and its speed profile does not show much of a decrease from the front to the rear that is typical of magnetic clouds at 1 AU. This almost flat profile might represent an evolutionary effect indicating that the cloud was "old" [*Farrugia et al.*, 1992, 1995b; *Osherovich et al.*, 1993b] and no longer rapidly expanding. On the basis of the cloud's average speed it is estimated that it left the Sun about 4.2 days earlier. Further studies of the speed profile are needed. A shock wave, observed ahead of the magnetic cloud by about 8 hours, occurred at 1042 UT on day 291 (October 18 at hour 10.7; this time is denoted by A in Figure 1). See Figure 5a for a preview of the detailed-IMF profile of the upstream shock, which was produced because the speed of the front boundary of the cloud relative to the solar wind, at least at some time, exceeded the ambient magnetoacoustic speed. The shock's characteristics are discussed below.

The magnetic cloud, whose beginning was at 1858 UT on day 291 (B in Figure 1) was being overtaken by a corotating stream. The stream apparently compressed the plasma and field at the rear of the magnetic cloud. A stream interface was seen at 2254 UT on day 292 (D_1, the start of region D) and characterized by an abrupt decrease in density, a similar increase in proton temperature (as seen in the proton thermal speed in Figure 1), and a peak in the magnetic field intensity. A corotating stream, indicated by the low density and high temperature, followed the stream interface. Wind was clearly in the stream after about hour 8 of day 293, when the speed and temperature were high, the density was low, and the magnetic field strength was average. The region between the (first) stream interface at 2254 UT on day 292 (D_1) and an apparent second interface at 0553 UT on day 293 (D_2, the end of region D) was complicated, owing to a second density peak and several large changes in magnetic field direction in that interval; this will be discussed further below in connection with Alfven waves seen in the fast stream. A distinct "boundary" within the magnetic cloud, showing a rapid rise in magnetic field intensity from ≈ 21 nT to ≈ 30 nT and modest changes in plasma parameters, was observed by Wind at 1751 UT on day 292 (C). A first impression is that this could be a corotating shock entering the rear of the magnetic cloud and driven by the fast stream trailing the cloud, but there are other possibilities, which we also discuss. Table 1 summarizes the times of these prominent boundaries.

Figure 2 supports the identifications given in Figure 1 concerning the nature of the regions in, and around, the magnetic cloud and shows various derived parameters. From top to bottom, Figure 2 shows the Alfven Mach number ($M_A = V/V_A$, where V_A is the Alfven speed, given by $B/(4\pi m_p N)^{1/2}$, where m_p is the mass of the proton), the proton plasma beta ($\beta = 8\pi NkT/B^2 = P_{Th}/P_B$), the proton thermal pressure (P_{Th}, dashed line) and magnetic pressure (P_B, dotted line), and their sum ($P_{Tot} = P_{Th} + P_B$), the dynamic pressure ($P_{SW} = m_p NV^2$), and an estimate for the instantaneous position (R_{MP}) of the subsolar magnetopause obtained from an assumption of approximate (static) pressure balance across the magnetopause boundary, from *Choe et al.* [1973]. M_A is variable but generally high (> 10) in all regions, except in the cloud where it is unusually low (~ 3). It may be surprising that there is such a small change of M_A at the "shock-like" boundary (C); notice that this event possessed very small

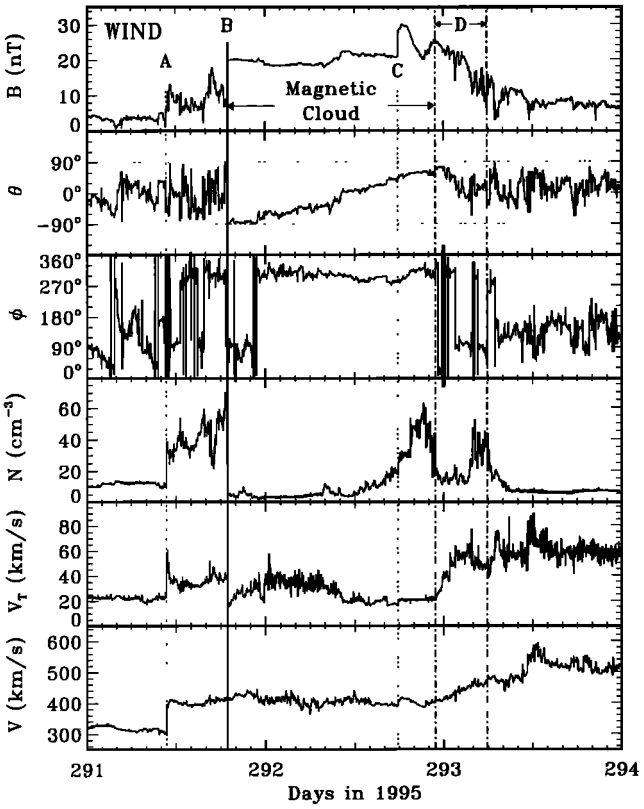

Figure 1. Magnetic field and plasma proton observations of the magnetic cloud and surrounding flows measured by Wind ≈ 175 R_E upstream of earth from October 18 (day 291), 1995 through October 20 (day 293) [*Burlaga et al.*, 1996]. The cloud starts at about 1900 UT (boundary B) of day 291 and lasts at least through day 292. The top three panels are the magnetic field in magnitude (B), latitude (θ) and longitude (ϕ), N is number density, V_T is proton thermal velocity, given by $\sqrt{(2kT/m)}$, and V is flow speed. The magnetic field is rendered in GSE coordinates. The vertical lines marked "interface" refer to the probable begin-time (considered boundary D_1) and end-time (D_2) of a stream interface bordering on the rear of the magnetic cloud.

changes in all plasma parameters giving a weak thermal pressure change also. Parameter β behaves similarly to M_A throughout the cloud, being high outside and low and very steady inside; β rarely went above 0.05 inside the cloud, except for the last few hours, and it reached values as low as 0.0045 for very short periods. The profile for β is especially revealing in helping to decide the locations of the magnetic cloud boundaries, along with M_A. It is usual for such a low β to occur in magnetic clouds generally. There is a very sharp discontinuity in all of these parameters at the start of the cloud and a broader discontinuity at the end, but at or near the start of the rise of proton β near the beginning of day 293 the spacecraft is probably leaving the cloud. As we show later, this time is also in agreement with the best end-time to choose for the fitting of the cloud as a force-free flux rope. We point out that the quantity R_{MP} is a rough measure of where the magnetopause is likely to be located based on the *Choe et al.*, [1973] relationship, which is strictly applicable for a static magnetopause boundary, and which we can only approximate in this case. Possible oscillations about the magnetopause's equilibrium position after a pressure front impinges upon it are not considered when using such a simple estimate.

From the fourth panel of Figure 2, notice how well that P_{SW} delineates the upstream shock and the front boundary of the magnetic cloud, especially the region between boundary C and parts of the stream-cloud interface, marked by D. Notice that P_{SW} is higher than average (~ 2 or 3 nPa) in all regimes except in the solar wind upstream of the shock (A), most of the cloud, and in the fast stream trailing the cloud. More is said on P_{SW} and R_{MP} in section 3.

2.2. Magnetic Cloud: Constant Alpha Force-Free Field Model

The magnetic field configuration in a magnetic cloud is approximately force-free [*Goldstein*, 1983; *Marubashi*, 1986]; a global view of the field lines speculated for such a structure out to 1 AU from the Sun is given in Figure 3b, from *Burlaga et al.* [1990], based on an analysis of multispacecraft data. The magnetic cloud's geometry is that of a nested set of helical field lines confined to a flux tube which is curved on the large scale (see a review by *Farrugia et al.* [1997]), i.e., a curved flux rope. The pitch angle of the helical field lines increases with increasing distance from the axis of the magnetic cloud, such that the field is aligned with the axis of symmetry at the position of the axis and perpendicular to it on the cloud's boundary (see Figure 3a). A useful analytical approximation for this field configuration is the static, constant-alpha (where $\mathbf{J} = \alpha\ \mathbf{B}$), force-free, cylindrically symmetric configuration [*Burlaga*, 1988], given by the Lundquist solution of $\nabla^2 \mathbf{B} = -\alpha^2 \mathbf{B}$, which results from assuming $\mathbf{J} = \alpha\ \mathbf{B}$ and the use of Maxwell's equations [*Lundquist*, 1950]. More accurate models must consider the possibility that magnetic clouds expand as they move away from the Sun [*Burlaga et al.*, 1981; *Klein and Burlaga*, 1982] and/or the possibility of a violation of cylindrical symmetry. Models of expanding magnetic clouds are reviewed by *Burlaga* [1995], and we note the recent work of *Farrugia et*

Table 1. Summary of Event Times

Day	Date	Time(HRMN, UT)	Symbol	Event Name
291	Oct. 18	1042	A	upstream shock
291		1858*	B	front boundary of magnetic cloud
292	Oct. 19	1751:04.26	C	internal "shock-like" feature
292		2254	D_1	stream interface
293	Oct. 20	0138		B_Z returns to normal values
293		0553	D_2	second stream interface ?

* Center time, of 4.0 min "thick" discontinuity.

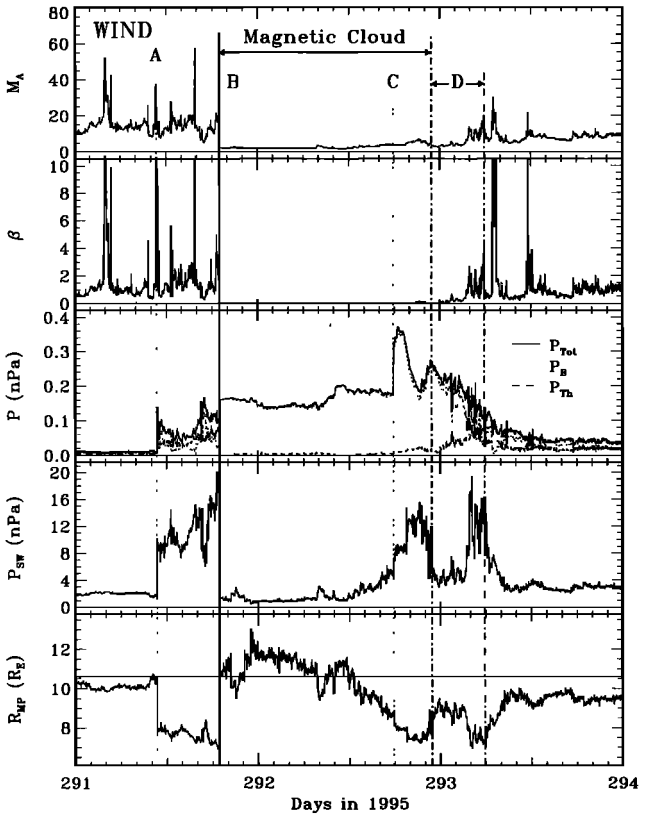

Figure 2. Derived physical quantities for the three days around the magnetic cloud (see Figure 1), where M_A is the Alfven Mach number, β is proton plasma beta, P is any one of three pressures as designated, P_{SW} is the ram pressure, and R_{MP} is the estimated subsolar magnetopause position as determined by R_{MP} = constant$(P_{SW})^{-1/6}$ [*Choe et al.*, 1973], where a constant 4% alpha particle contribution [*Hundhausen*, 1995] was added to the solar wind proton density. The horizontal line in the R_{MP} panel (bottom), at 10.6 R_E, indicates an average value for R_{MP} as determined by [*Fairfield*, 1971], for comparison. (Note that none of the parameters were displayed to start at zero.) The end of the magnetic cloud may occur where there are almost simultaneous increases in M_A, β, P_{SW} within the probable interface, which is also at a large change of latitude of the magnetic field, θ, as seen in Figure 1.

al. [1992, 1995a, b]; *Osherovich et al.* [1993a, b, 1995]; *Vandas et al.* [1995, 1996], and *Kumar and Rust* [1996]. Magnetic clouds can interact with other flows [*Burlaga*, 1995]; as mentioned, the magnetic cloud that is the subject of this paper was being overtaken by a corotating stream. The theory of such interactions remains to be developed. A detailed analysis of observations from two spacecraft of the magnetic cloud of February 16 - 17, 1980, showed that magnetic field lines can extend continuously from the Sun through the magnetic cloud to the lobe of the geomagnetic tail [*Farrugia et al.*, 1993c].

We fit the Lundquist solution to the field observations using the method of *Lepping et al.* [1990] and give the results in Figure 4, which is presented in GSE coordinates. The least squares fit is made to unit normalized (initially) magnetic field data for the 30-hour interval beginning at 1859 UT of day 291 (see B in Figures 1 and 2). (A simple linear scaling of the model field magnitude to the observed field intensity is done after the least squares fit, as a final step.) As discussed in the next section, the front boundary is well defined, but there is some uncertainty in the position of the rear boundary. The rear boundary could have occurred as early as 2254 UT of day 292 (the first interface marked in Figure 1 as D_1) or as late as 0138 UT of day 293 when the elevation angle drops abruptly to near 0°. The top three panels of Figure 4 show that the fit (solid curves) describes the observations (dots) of the three components of the magnetic field rather well, which is true also for the field angles θ and φ, where the magnetic cloud's end-time was chosen to be 0000 UT of day 293. The "reduced"-chi-squared to the fit, $\chi^2/(3N - n)$, where $N = 30$ is the number of hour-average points and $n = 5$ is the number of parameters in the fit, is only 0.015 for this case; this quantity is dimensionless since the magnetic field was unit normalized up to this point. Extending the fit another 2 hours increases the reduced-chi-squared value to about 0.03, suggesting that the former (shorter, 30 hour) interval better identifies the magnetic cloud. Also this end-point appears to be in temporal agreement with the change of proton plasma β as

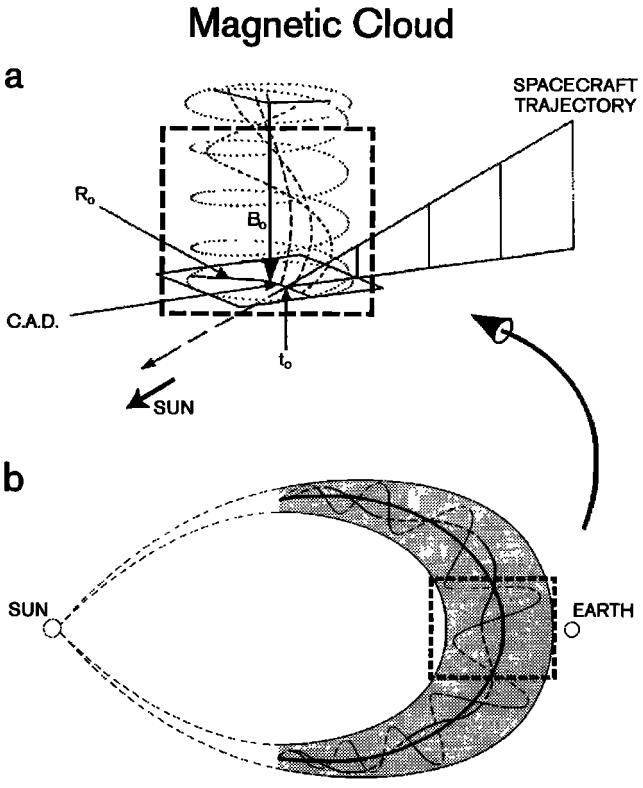

Figure 3. (a) Idealized cylindrically symmetric force free flux rope, representing the magnetic cloud as observed by a spacecraft traveling through it (relative to the cloud's motion) and showing the relevant model parameters; other model parameters are rope handedness and the attitude of the cloud's axis, usually given by its longitude and latitude. The model is thought to be a reasonable local approximation of the global cloud. (b) Shows a sketch of the cloud's envisioned global geometry (i. e, on a 1 AU scale in this case) and the helical field lines within, shown here in projection. The sketch, drawn by A. Burlaga, is reproduced from *Burlaga et al.* [1990].

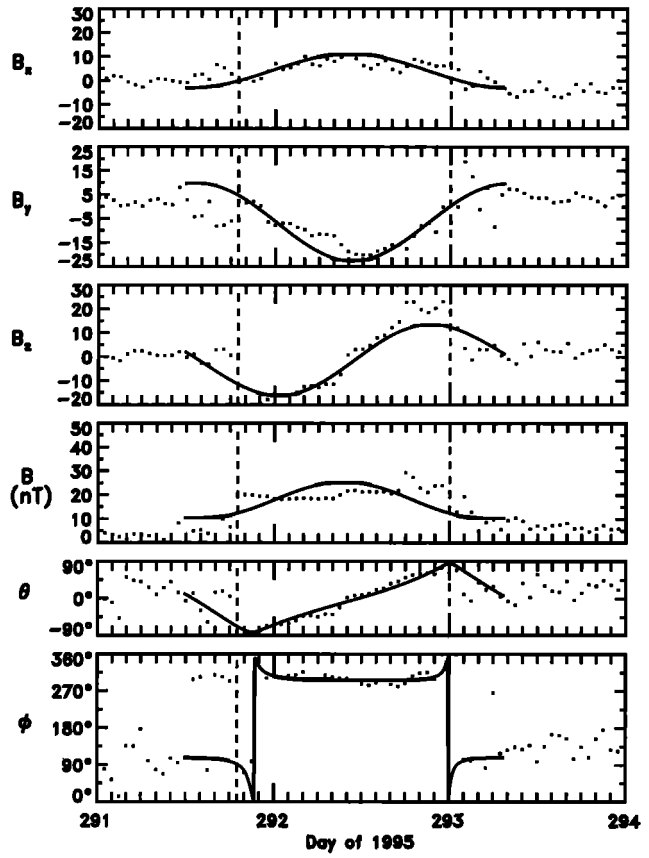

Figure 4. A comparison of the magnetic field (dots) and a force-free flux rope model (solid curve; see text) during the passage of the magnetic cloud, given in terms of Cartesian components $B_{x,y,z}$ (in GSE coordinates) and also in magnitude B, latitude, θ, and longitude, ϕ, respectively. The vertical dashed lines represent the beginning (hour 19 of day 291) and end (hour 0 of day 293) times of the cloud, where the end-time is not as certain as the begin-time. From the model: the axis of the magnetic cloud is $\phi_A = 291°$, $\theta_A = 12°$, the helical field is right-handed, the diameter is 0.27 AU, and the relative closest approach distance in terms of the estimated radius is 0.081.

a cloud boundary indicator, as shown in Figure 2. Notice also that it is where the magnetic field becomes almost exactly "northward," and we know [*Lepping et al.*, 1990], that this is consistent with a cloud whose axis is approximately contained in the ecliptic plane and observed by a spacecraft that passes close to the cloud's axis, and as we will see this cloud fits those conditions. (This arises from the fact that in the model the boundary of the cloud must occur where the magnetic field becomes purely azimuthal.) However, the exact end-point was not as evident as hoped. The fit curve in Figure 4 is deliberately shown outside of the estimated end-points of the cloud (the vertical dashed lines in Figure 4), as well as for the region of the cloud itself, in order to observe the degree of departure of the fit curve from the observations outside. This departure is very clear before the magnetic cloud in almost every parameter of Figure 4, but less so after the cloud, consistent with our difficulty in determining the cloud's exact end-point. The variation of the magnetic field's intensity ($|B|$) is not modeled very accurately, in part because of the cloud's interactions: at the front boundary with the upstream solar wind, which it was overtaking, and at the rear with a corotating stream that produced an enhancement of the magnetic field by compression, but possibly also because of the age of the cloud, and probably because of the influence of event C, a shock-like structure. Theoretical studies are needed to explain this profile. The bottom two panels of Figure 4 show that despite the unusual magnetic field strength profile the constant-alpha force-free model provides an excellent fit to the variation of the direction of the magnetic field, indicating that the "force-free flux rope" geometry was not destroyed by the interaction.

The axis of the magnetic cloud is estimated to be in the direction $\phi_A = 291°$, $\theta_A = -12°$, i.e., close to the ecliptic plane and 69° from the radial direction, which is a rather typical observed orientation for magnetic cloud axes [*Lepping et al.*, 1990], and the cloud's helical magnetic field was right-handed. The spacecraft nearly intercepted the axis of the magnetic cloud, Y_0/R_0 being 0.081, where Y_0 is the closest approach distance (C.A.D.) to the magnetic cloud and R_0 is the cloud's radius; see the top sketch in Figure 3. This result is consistent with the observations of an extended interval of negative B_Z within the first half of the cloud, followed by an interval of similar length of positive B_Z giving an overall nearly symmetric B_Z profile inside the cloud. B_0 is estimated to be 25.6 nT, higher than the value of the field at the closest approach point to the axis, as seen in panel 4 of Figure 4. The estimated diameter of the magnetic cloud resulting from the fit was 0.27 AU, which is typical for magnetic clouds at 1 AU. However, the duration of the passage of the magnetic cloud (≈ 30 hours) is relatively long owing to its moderately low speed, so that any associated geomagnetic effects should be prolonged.

2.3. Front Boundary of the Magnetic Cloud

The front boundary of the magnetic cloud at 1858 UT on day 291 (boundary B in Figure 1 and shown in detailed IMF in Figure 5b) was well defined. The magnetic field strength increased, the magnetic field direction rotated southward, the density decreased by a large amount, and the temperature decreased. The large abrupt changes in the field and plasma parameters suggest that the boundary was a tangential discontinuity in the MHD limit. Figure 5b shows that this boundary was a magnetic hole, i. e., a small-scale magnetic structure in which the field strength is low and across which the total pressure was approximately constant. This is not an unusual feature at the front boundary of a magnetic cloud [see, e.g., *Burlaga*, 1995]. If one takes a 4-min analysis-interval at the boundary, with beginning and end times (of the magnetic hole) at 1856:19.5 and 1900:16.5 UT, respectively, the magnetic field direction rotated through 176° in a plane. A variance analysis using the unnormalized magnetic field vectors shows that the normal to this plane had the direction $\phi_n = 184°$, $\theta_n = -3°$. This was a well-determined normal with an intermediate to minimum eigenvalue ratio of 25 (over 80 vectors) using 3-s averages. Recall that the axis of the magnetic cloud was approximately $\phi_n = 291°$, $\theta_n = -12°$. Hence the angle between the longitude of the normal to the front boundary of the magnetic cloud and that of a normal to its axis is only 17°; it is legitimate to consider only longitudes, since the latitudes are so close to zero. The component of the magnetic field normal to the plane of rotation of the field (B_n) at the front boundary was 1.3 nT ±

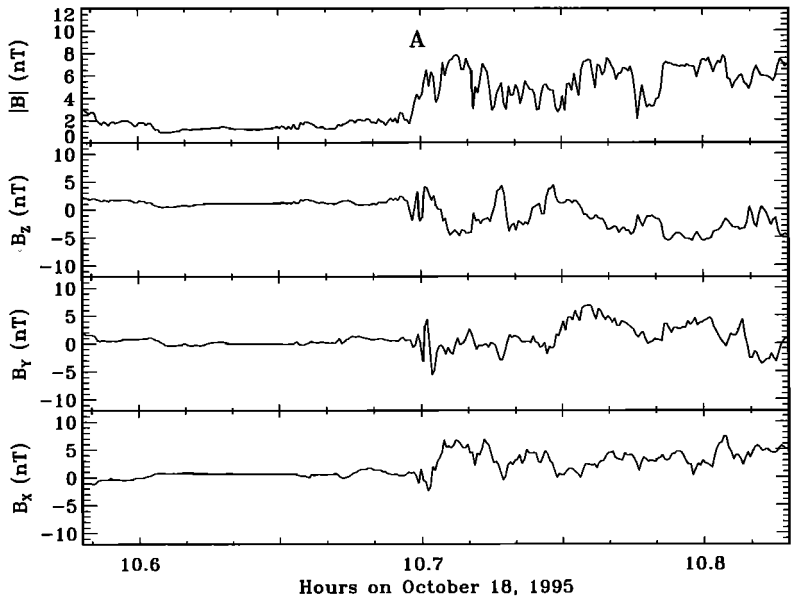

Figure 5a. Three-second averages of the magnetic field in angle format as in Figure 1 for the region around the interplanetary shock in front of the magnetic cloud; boundary A is marked in Figures 1 and 2.

2.0 nT (for a two-sigma uncertainty), and since $B_n/|B|$ was 0.065, where $|B|$ was 19.9 nT, this is consistent with a B_n of zero, providing additional evidence that the boundary was a tangential discontinuity.

2.4. Interaction of the Magnetic Cloud and a Corotating Stream

An apparent stream interface, which might correspond to the rear boundary of the magnetic cloud, was observed at 2254 UT of day 292 (D_1 in Figures 1 and 2) behind a region of high density and strong magnetic fields. There appears to be a second stream interface at 0553 UT of day 293 (D_2) following a second enhancement in intensity. The presence of two enhancements is unusual, and should be studied in future analyses of this event. A series of large directional discontinuities was observed in the region between these two interfaces. A variance analysis was performed on the magnetic field in the period between 0115:30 and 0914:30 UT of day 293, about 8 hours duration, which encompassed seven major and many moderate discontinuities (a judgement based on the size of the field angle change) and the normal to this "boundary" was shown to be $\phi_{D'} = 188°$ and $\theta_{D'} = 29°$. It is interesting that several of the discontinuities within this broad region yielded similar results when their field variation is analyzed through variance analysis. For example, a very well defined but broad directional discontinuity occurring between 0338:23 and 0354:14 UT (16-min duration) on day 293

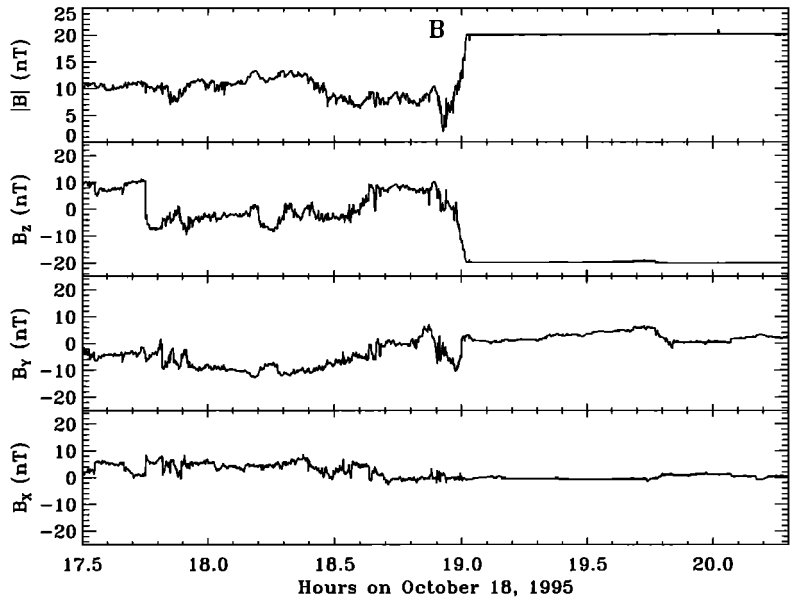

Figure 5b. Three second averages of the magnetic field at the beginning of the magnetic cloud, as discussed in the caption of Figure 2. Boundary B is marked in Figures 1 and 2.

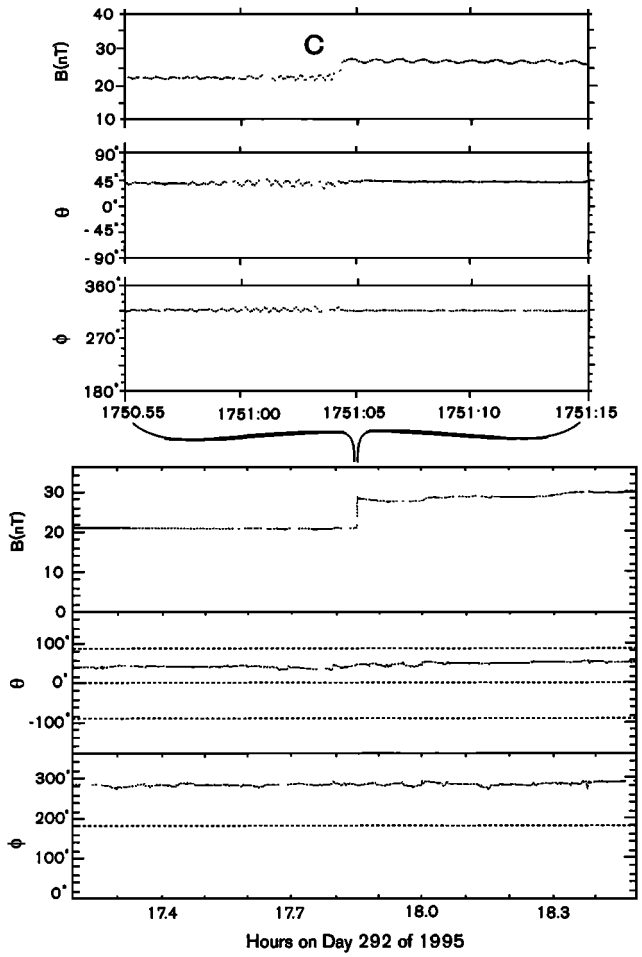

Figure 5c. Three second averages of the magnetic field for the region around the interplanetary shock inside of the magnetic cloud, as shown by C in Figures 1 and 2. The inset at the top provides the very highest time resolution averages available from the spacecraft at this time, one average every 0.092 s, showing the shock ramp to be centered at 1751:4.26 UT and that it occurred in about 0.184 s from prior ramp minimum to post ramp maximum.

yielded a normal given by $\phi_D = 194°$ and $\theta_D = 37°$, which differs by only about 9° from the normal associated with the overall 8-hour period noted above.

Figure 6 shows a hodogram of the magnetic field for the 16-min interval in variance coordinates showing the obvious arc of a circle (for a nearly constant intensity field) given by the tip of the field vector in the B_i-B_j plane, where the i, j, and k subscripts represent the maximum, intermediate, and minimum eigenvalues, respectively. The hodogram in the B_i-B_k plane reveals a very small average component of the total field normal to the discontinuity plane ($\langle B_k \rangle$), consistent with zero when compared to the rms-deviation of the B_k component, i.e., consistent with the discontinuity being a tangential type. The field rotated through 207° as the discontinuity passed the spacecraft which is readily seen in the left panel of Figure 6. The mid/min eigenvalue ratio of 12 and the large discontinuity angle of 207° ensured that the discontinuity normal was well determined. Very likely the direction of the normal was being strongly influenced by the presence of the magnetic cloud's rear boundary, since draped magnetic fields would be important at the boundary. We say this because the cloud's boundary in the ecliptic plane (according to a simple cylindrical symmetric model) is consistent with this locally determined "boundary normal" within about 7°.

The magnetic cloud-stream interaction region is unusual, and its nature is not likely to be determined fully from single spacecraft observations, as have been considered here. Nevertheless, we speculate on it. One possibility is that a compound stream followed the magnetic cloud and the two stream interfaces would correspond to the two corotating streams. A second possibility is that a corotating stream was interacting with the heliospheric plasma sheet, in which case the multiple directional discontinuities might represent crossings of the heliospheric current sheet. A third possibility is that a single corotating stream interacted with the magnetic cloud and produced an instability that formed a complex boundary. A fourth is that the corotating stream interacted with the wake of the magnetic cloud. And a fifth is that its structure was partly the result of an independent event at the Sun. This last possibility is based on the peculiar aspects of the shock-like feature (boundary C) inside the magnetic cloud seen not far from the rear boundary of the cloud (D_1) where the stream interaction was taking place. Other multispacecraft studies, compositional analyses, detailed discontinuity analyses, energetic particle observations, and solar observations might help to define the nature of the interaction that is presently beyond the scope of this paper.

The stream's interaction with the magnetic cloud may have directly created the discontinuous field rise, internal to the cloud, seen at 1751 of day 292 UT (C; given in high-resolution IMF data in Figure 5c). If this ramp was indeed representative of a corotating shock surface, it then presumably would have entered the rear of the cloud, and we believe that this is a possibility [*Burlaga et al.*, 1996]. However, as pointed out, this "shock" may have been born at the Sun, temporally or spatially independent of the magnetic cloud's origin, because it is estimated to have a surface

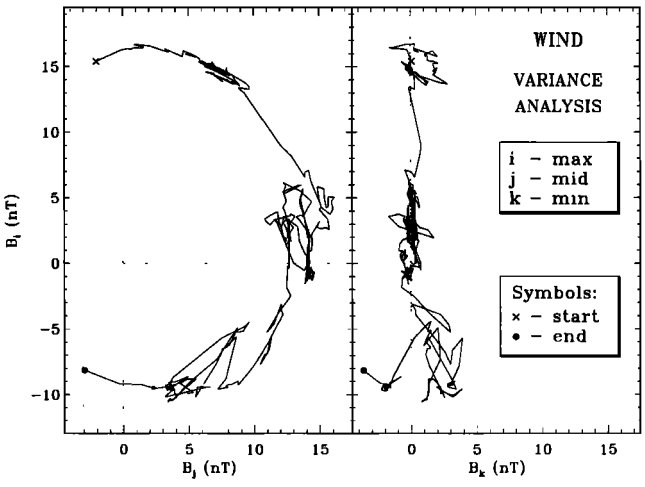

Figure 6. The hodograms for a prominent magnetic field discontinuity in the post-cloud stream interface region over the 16-Min interval 0338:22 to 0354:13 UT of day 239 (October 19), where the B_i-B_j plane is the max-mid variance plane, and the B_i-B_k plane is the maximum-minimum variance plane, as indicated. Notice that the average of the field in the minimum variance direction (k), which was 0.30 nT, is consistent with zero for the associated rms, 1.26 nT. There were 318 3-s points across this discontinuity.

normal not in agreement with what would be expected from a simple direct impact of a corotating stream (or compound stream) with the cloud. In section 2.5 we discuss the analysis of this shock-like feature.

Just beyond the stream interface with the magnetic cloud, i.e., over the days 293 to 294, a very clear anticorrelation was seen between large perturbations in the magnetic field and solar wind velocity perturbations with periods around 1/2 hour. It was shown that the relationship, $\Delta\mathbf{B} \propto \pm(4\pi m_p N)^{1/2}\Delta\mathbf{V}$, indicative of Alfvenic fluctuations, where the sign was negative in this case (indicating outward propagation) was reasonably well demonstrated by these perturbations. This is shown in Figure 7, where specifically $\mathbf{A} \equiv \mathbf{V}/(4\pi m_p N)^{-1/2}$. A quantitative measure of the quality of the correlation is given by the correlation coefficients, $R_{x,y,z}$, also presented in the figure. With the moderately large correlation coefficients obtained, and a large number (1609) of data points, large-amplitude outward propagating Alfven waves are inferred to be occurring on October 20 and 21. Large-amplitude Alfvenic wave fluctuations are commonplace in the region where a fast stream overtakes a slower stream, but to our knowledge these are the first observations of Alfven waves in a magnetic cloud-stream interface. The interaction of these Alfven waves with the magnetic cloud should be investigated further, since their presence may contribute substantially to the cloud-stream interaction. See *Tsurutani et al.* [1995a] for a discussion of large-amplitude IMF fluctuations in corotating interaction regions, based on Ulysses observations for regions at midlatitudes.

While it is conceivable that the observed Alfven waves could have been generated by the stream-stream interaction, a more likely explanation is that they are intrinsic to coronal hole high-speed streams. The declining phase of the solar cycle is dominated by large coronal holes, which remain relatively fixed on the Sun [*Tsurutani et al.*, 1995b]. The fluctuating (about zero) B_Z fields comprising these Alfven waves are expected to cause a type of auroral electrojet activity called high-intensity, long duration, continuous *AE* activity (HILDCAAs) [*Tsurutani and Gonzalez,* 1987; *Tsurutani et al.*, 1995b]. While the *AE* index is not available at this time, we do show below the 3-hourly planetary *Kp* index (see Figure 9), which also responds to auroral activity, though not exclusively to it.

Further examples of a magnetic cloud interacting with a solar wind stream are given by *Behannon et al.* [1991].

2.5. Analysis of the Shock-Like Structure Internal to the Magnetic Cloud

We start the analysis of this feature by assuming it is an MHD fast shock, because of its obvious (fast) shock-like characteristics, as presented in Figures 1 and 2, and estimate a shock surface normal ($\mathbf{n}_s$). The normal was determined by several methods described by *Abraham-Shrauner* [1976]. Probably the most reliable normal estimate was from the results of the so-called mixed data method (MD3), where the use of the magnetic field difference and solar wind velocity difference across the shock were employed using 10-min averages of these quantities on each side. The normal was estimated to be $\phi_C = 128°$ and $\theta_C = 25°$. This direction makes an angle of only 21° from the direction antiparallel to the magnetic cloud axis (see estimate of axis above). This direction is far from the radial direction from the Sun, which

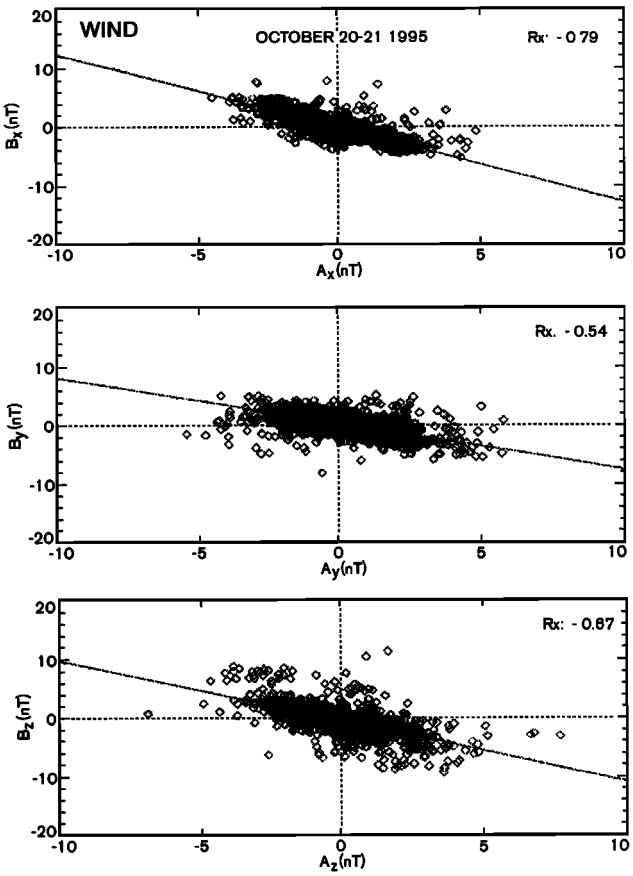

Figure 7. Component plots in GSE coordinates of the IMF versus A, which is the normalized solar wind velocity (i.e., the velocity V divided by the factor $(4\pi m_p N)^{-1/2}$). The $R_{x,y,z}$ are the correlation coefficients for the three straight-line fits, and there were 1609 points used in the analysis. The analysis interval was that immediately following the stream-magnetic cloud interface: October 20 - 21.

would be a more expected result, especially under the presumed circumstance. The estimated shock velocity in the solar wind frame of reference was 137.4 km/s, and since the solar wind speed along the normal was 200.6 km/s, the speed of the shock as seen by the spacecraft was slow, V_s = 338 km/s; we stress, however, that the shock normal is far from the solar wind's radial direction. As shown in Figure 5c (inset at top) the ramp for this field change is very thin; it passed the spacecraft in about 0.184 s, or in two "sample times." (Strictly speaking, these represent two on-board averages at this time.) Using the shock speed (338 km/s) along the normal in the spacecraft frame of reference, the ramp thickness was estimated to be only 62 km. This small value is consistent with the structure being truly a shock wave, and in fact, is thinner than most predictions for collisionless shock ramps [*Leroy et al.*, 1982]. It could conceivably depend on the electron plasma frequency rather than on any proton parameter (see, for example, remarks by *Goodrich* [1985] concerning this issue, and a possible example of such a very thin shock ramp having an estimated thickness equal to two electron inertial lengths [*Newbury and Russell*, 1996]). The high-resolution data show some very prominent oscillations preshock and postshock; the preshock waves had a period in the spacecraft frame of about 0.46 s, and the clearly

monochromatic downstream waves, which for the most part decayed in amplitude in about 27 s, had a period of about 1.0 s. These 1-s waves reappeared intermittently after the 27 s but at much lower amplitudes and apparently lost their monochromatic characteristic. The latter waves are seen (Figure 5c) more markedly in the intensity of the field, than in direction, and are predominantly in the Z component (GSE) and to some extent in the Y component. They are presently under investigation.

We now present specifics on the shock fitting analysis. The shock normal was calculated using velocity and magnetic coplanarity and three mixed methods [*Abraham-Shrauner*, 1976]. With the exception of the velocity coplanarity, all of the methods yielded very similar results increasing our confidence of a well-estimated normal. Then all of the obtained normal directions were used to calculate the downstream magnetofluid parameters based on the upstream parameters and the full MHD jump condition equations. If the discontinuity is truly a shock and the normal is selected properly, the calculated downstream parameters should match the observed value. The closest correlation was obtained with the mixed method 3. Only the observed total downstream temperature showed a significant discrepancy. Next, we made the assumption that the shock is exactly perpendicular (based on the very small directional change of about 3° in the magnetic field across its ramp and on its thinness), and we repeated the MHD comparison to directions in the plane perpendicular to the upstream magnetic field, spaced out by 10° increments. The direction yielding the best correlation was about the same quality as the mixed method 3 normal fit. These two best normal directions are 30° apart. Finally, the plane defined by these two directions was explored. The best quality fit was found for a direction approximately half way between the two previous best solutions. For this final "best" direction the magnetic field was fitted to less than 10% discrepancy and the velocity of the order of 1%, which are as good as the best fit results of other fitted shocks.

Assuming that boundary C was a bona fide fast mode shock, we calculated its magnetosonic Mach number upstream and downstream of the ramp, where both proton and electron temperatures were considered. The upstream fast mode Mach number was 2.7, a reasonable value for such an assumed shock. The downstream fast mode Mach number was 1.96, which is not a permissible value for such a shock. This discrepancy caused serious concern and brought us to doubt the interpreted nature of this feature. There are, in fact, two serious physical shortcomings concerning this interpretation: (1) The temperature is predicted to cool through the shock by the MHD equations which is contrary to the observations; and (2) the shock speed resulting from the analysis would result in the solar wind speeding up through the shock (this is related to the downstream Mach number problem) which violates the entropy increase requirement of MHD shocks. Therefore this feature cannot be considered to be a proper shock, but it shows some similarity to one. Hence it very well might be a pressure pulse on the way to steepening into an MHD shock.

Because of our inability to obtain a fully consistent picture for this shock-like feature, and due to the peculiar estimate of its surface normal, we tested other possibilities for its character. And, if indeed it approximates a bona fide shock (a wave steepening into an MHD shock), we still questioned the reasonableness of its estimated normal and speed ($\mathbf{n}_s$ and V_s). Fortunately, an independent check of these was possible, because parts of the magnetic cloud were observed by the Geotail spacecraft (D. Fairfield, private communication, 1996), which was close to the Earth's bow shock. The bow shock oscillated past the spacecraft numerous times, and fortuitously the shock-like ramp within the magnetic cloud was observed outside of the bow shock at 1823:02 UT on October 19. A time delay check for this ramp was then possible using the previously estimated shock surface normal and speed. Assuming that the shock surface was sufficiently planar over the dimensions of interest and using the expression $(\mathbf{n}_s \cdot\cdot \mathbf{V}_s) \equiv V_\perp = \mathbf{n}_s \cdot\cdot \Delta\mathbf{R}/\Delta t_s$, where Δt_s is the delay between the observations of the shock-ramp at the two spacecraft, and likewise $\Delta\mathbf{R}$ is the vector displacement between them, we were able to check the reasonableness of the estimated shock properties, $\mathbf{n}_s$ and V_s. This led to a Δt_s of 32.4 min, in excellent agreement with the observed delay Δt_s(obs) of 32.0 min, supporting the estimated shock normal and speed. However, we considered still another possibility: that this feature may be a tangential discontinuity (i.e., a field structure frozen into the solar wind) having a surface normal (as yet unknown) probably very different from $\mathbf{n}_s$. (Variance analysis did not allow a unique determination of the normal to such a discontinuity, because there was very little change in direction of the field across it.) Then using the appropriate expression $(\mathbf{n}_{TD} \cdot\cdot \mathbf{V}_{sw})\ \Delta t_s\ (\text{obs}) = (\mathbf{n}_{TD} \cdot\cdot \Delta\mathbf{R})$, which is approximately the same as $V_{sw}\ (\mathbf{x} \cdot \mathbf{n}_{TD})\ \Delta t_s\ (\text{obs}) \approx |\Delta\mathbf{R}|\ (\mathbf{r} \cdot \mathbf{n}_{TD})$, where $\mathbf{x}$ is a unit vector along the x axis(GSE) (assumed to be opposite the direction of the solar wind flow), and $\mathbf{r}$ is a unit vector along $\Delta\mathbf{R}$ (which is aligned with $\mathbf{x}$ within 5°), gives V_{sw} (est) $\approx |\Delta\mathbf{R}|/\Delta t_s$ (obs), to a good approximation. (Notice that V_{sw} (est) is fortunately independent of $\mathbf{n}_{TD}$, under these assumptions.) Using values for the quantities that we know well ($|\Delta\mathbf{R}|$ and Δt_s(obs)) in this expression yields an estimated value for the solar wind speed for this assumed tangential discontinuity. The result is a speed (V_{sw} (est)) of 539 km/s. However, the observed solar wind speed was actually about 400 km/s at the time, giving an unacceptably large discrepancy of 35% and indicating that the ramp was not likely a tangential discontinuity. Other physical checks were made of the character of this ramp, including the possibility of it being a rotational discontinuity, and the case for a shock-in-formation is the best of the acceptable candidates. We now present a summary of the case for the shock-like feature, in comparison to the cases for a tangential or rotational discontinuity:

Case against a tangential discontinuity (TD): (1) There is a significant pressure imbalance across the "boundary"; (2) boundary is too thin for a TD; and (3) to have a good correlation with Geotail's observation time would require an unreasonable solar wind speed, 35% higher than that actually observed.

Case against a rotational discontinuity (RD): (1) There is a very large |B| jump which would require an extremely (and unbelievable) anisotropic plasma; (2) the same comment holds for the plasma density; (3) the boundary is too thin for an RD; and (4) the Geotail time correlation and plausible speed would necessitate a normal significantly rotated from the radial direction.

Case for a shock-like character: (1) The boundary (ramp) was estimated to be thin; (2) there was consistency among

the various trial estimates of the surface normal; (3) the time delay estimate to Geotail was excellent; (4) the MHD jump conditions fit the observed density, velocity, and magnetic field conditions. (Only the temperature measurements are in conflict.); and (5) the observed sense of change of the observed magnetofluid parameters is consistent with a fast forward shock.

Hence a shock-like identity for the discontinuity at boundary C is the most acceptable, at least of those types considered.

3. Events as Triggers for Geomagnetic Activity

A major geomagnetic storm and associated aurorae were produced by the extended interval of negative B_Z in the front part of the magnetic cloud [*Farrugia et al.*, 1996b]. As the magnetic cloud moved past the earth, the magnetic field slowly rotated northward giving an extended interval with positive B_Z in which the geomagnetic activity subsided. Near the rear of the magnetic cloud the northward fields were further enhanced by the internal "shock" and the interaction with the corotating stream, resulting in a return of the magnetosphere to a quiet state. Figure 8 shows, from top to bottom, the clock angle, ψ (i.e., the polar angle between the Z axis(GSM) and the magnetic field of interest as projected into the *Y-Z*(GSM)-plane), the so-called Akasofu ϵ parameter, and the VB_S parameter, where V is the speed of the solar wind and B_S is defined below. The ϵ-parameter is defined as the integrated Poynting flux of the solar wind into the magnetosphere, given by $\epsilon = VB^2 l_0^2 \sin^4(\psi/2)$ (where l_0^2 is an effective cross-sectional empirical constant for the magnetosphere and where l_o is set equal to 7 R_E) [*Perreault and Akasofu*, 1978; *Akasofu*, 1981]. VB_S is the rectified electric field, which is defined as $-VB_Z$ if the B_Z component of the ambient field is < 0, and VB_S is 0 otherwise. Both parameters have been used in the past as measures of the solar wind coupling to the magnetosphere and are considered to be good predictors of substorm activity [see *Baker et al.*, 1984]. A detailed discussion of the geomagnetic activity is beyond the scope of this paper, which is principally concerned with the description of the solar wind events of these 3 days which may act as interplanetary triggers of geomagnetic activity. A related paper on the geomagnetic consequences of these interplanetary events is by *Farrugia et al.* [1996b]. However, we point out a few salient features.

The continued forcing of the magnetosphere by the magnetic cloud during the cloud's negative B_Z interval (i.e., from the cloud's front boundary to about 1034 UT for the ϵ profile) led to a number of substorms as monitored by auroral zone magnetometers [*Farrugia et al.*, 1996]. These substorms occurred during the major magnetic storm mentioned above. All storm activity subsided, and the ring current decayed during the time of the northward field in the cloud, only to resume, albeit at a lower intensity, during the fast stream, in which there were outward propagating B_Z fluctuations. This magnetospheric activity was correlated with the sporadically enhanced values of both substorm indicators ϵ and VB_S, evident in Figure 8. Figure 9 shows the *Kp* index for the three days of interest in relation to the ϵ parameter, with proper account of the time delay from Wind to Earth for ϵ the temporal placement. *Kp* reached a maximum value of 7-

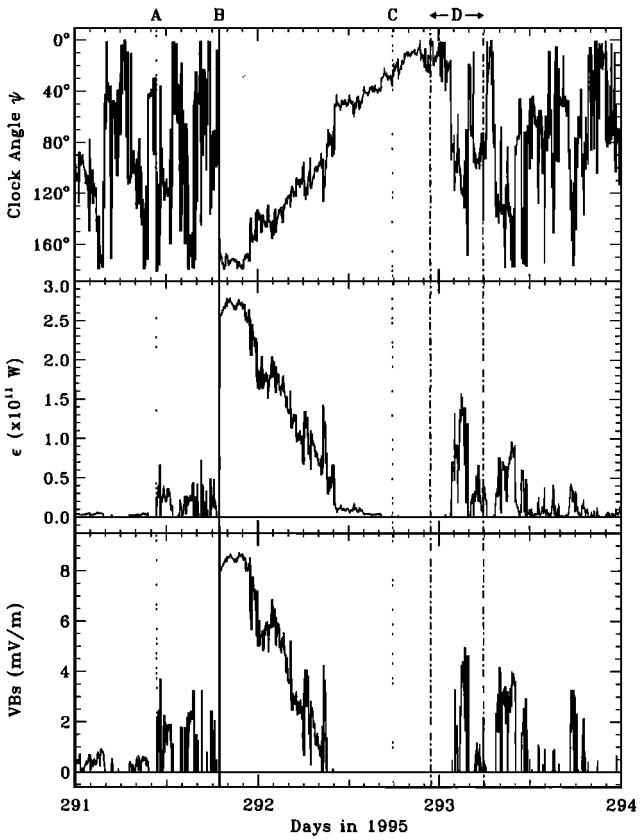

Figure 8. (top) Clock angle ψ of the magnetic field measured from the +*Z* direction in the *Y-Z* plane in GSM coordinates. (middle) The integrated Poynting flux in the solar wind (see text). (bottom) The absolute value of the induced electric field, as defined by $-VB_Z$, where zero is assumed for all northward fields.

during the continuously southward pointing cloud-field just before the end of October 18 (day 291). The values reached by various substorm indicators, including *Kp* [*Farrugia et al.*, 1996], became lower and less continuous later in the cloud than during the early part of its passage, partly because magnetic field strengths were lower then (see Figure 1) and partly because ψ fluctuated strongly, as seen in Figure 8 (top). Of course, there was a diminution of *Kp* during the northward pointing phase of the cloud-field, starting just before midday on day 292. It is also interesting to note that ϵ (and VB_S) shows significant activity early on day 293, in the stream interface region, as described above, despite the fact that the field then is at a lower intensity than during the cloud period and $|B_Z|$ is weaker. This activity is obviously due to the fact that again B_Z becomes negative, and $|B|$ and V are still significant; in fact, V has increased. We stress that the *Kp* index, while not an ideal indicator of the strength of the ring current, does also respond to ring current enhancements (see a discussion on this by *Gonzalez et al.* [1989]). Using preliminary *Dst* readings *Farrugia et al.* [1996] show that there were, in fact, two storms, one major (the first) and one moderate (the second), but with different causes, as explained.

We now want to call attention again to the quantity R_{MP}, given in the bottom panel of Figure 2, which gives a rough estimate of the variation of the magnetopause stand-off distance predicted by using the *Choe et al.* [1973] (static

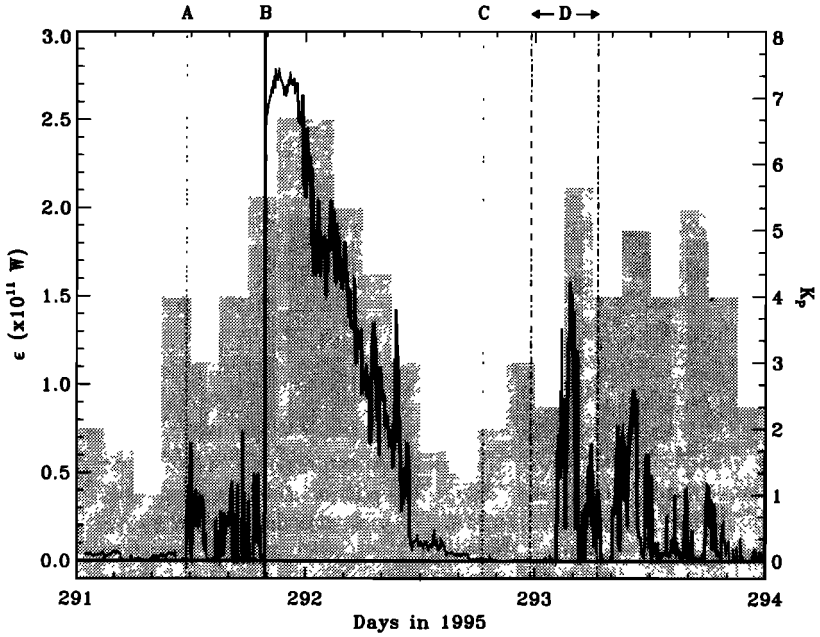

Figure 9. The shaded block diagram represents the (3-hours/estimate) *Kp* index for 3 days starting at 0000 UT of October 18, 1995. The solid curve is the ϵ parameter from Figure 8, except now shifted in time for Earth observation as delayed by solar wind convection time (which was on average 45 min) according to the actual speed of the solar wind.

pressure) relationship. Since it is a static pressure approximation, it therefore does not account for the results of solar wind ram pressure (P_{SW}) changes which would accelerate the boundary, nor does it account for any delayed motion of the boundary resulting from any earlier changes, for example. Also, we do not account here for any possible magnetic merging at the boundary which is considered to cause a lesser effect than significant ram pressure changes, as far as bulk positioning of the boundary is concerned. Although the estimation of R_{MP} made in this manner should be applied cautiously, it nevertheless should give an approximation to the dramatic variations in size of the magnetosphere expected during this magnetic cloud passage; it was based on the determination of P_{SW}, given by the next-to-last panel of Figure 2. The R_{MP} estimate shows a variation from about 10.5 R_E, which is close to an average magnetopause standoff distance of 10.6 R_E [*Fairfield*, 1971], just before the interplanetary shock at boundary-A, to a very compressed value of ~ 7.5 R_E in the cloud's sheath region, between A and B. After the passage of the front boundary of the magnetic cloud at point B, R_{MP} reaches inflated values as high as 12 or 13 R_E to about midday of day 292. It then steadily decreases back to a compressed value of about 7.5 R_E at the end of the cloud, back to an intermediate and typical value (about 9.5 R_E) in the early interaction region (D_1), and finally, again, back to nearly typical values after midday of day 293, similar to early on day 291. This reveals a series of dramatic compressions and inflations, sometimes occurring very abruptly, especially at the upstream shock ramp (A) and at the front boundary (B) of the magnetic cloud. These changes in size of the magnetosphere are expected to have important geomagnetic consequences. For example, during a sharp decreases in R_{MP} the magnetospheric field will be compressed and the *H* component of the Earth's field will increase, and conversely for a sharp increase in R_{MP}. Variations in R_{MP} are expected to cause instabilities and or waves traveling along the magnetopause surface [*Lepping and Burlaga*, 1979] and set up various pulsations of the geomagnetic field [see, e.g., *Song et al.*, 1988; *Farrugia et al.*, 1989], some of which may be directly coupled to the magnetopause motions. To these we add the possibility of mode-mode wave coupling, i.e., compressive MHD mode coupling to the Alfven mode, which then travels to the ionosphere, exciting motions there through the field aligned currents that the MHD Alfven mode carries, as discussed, for example, by *Southwood and Kivelson* [1990].

Finally, we point out that theoretical modelling predicts that, upon the magnetic cloud's interacting with the Earth's bow shock and magnetosheath, the condition of a low M_A within the cloud (recall that it was typically ~3 (Figure 2)) should enhance control of the shocked solar wind flow by the cloud's magnetic field in the magnetosheath, leading to wide depletion layers there [see, e.g., *Farrugia et al.*, 1995a].

4. Overall Event Geometry

Table 2 and Figure 10 summarize the geometrical associations of the structures constituting the overall three-day magnetic cloud - stream interaction event. These associations are based on the results of the magnetic cloud fitting analysis and four separate surface normal studies, i.e., for both cloud boundaries, front and back, and the "two" interplanetary shock fronts, all given in Figure 10 in terms of longitudes (in GSE coordinates) of the boundary normals. (Recall that the latitudes of these normals are not very high, allowing a meaningful two dimensional representation.) Despite the complexity of the interplanetary stream-cloud interaction, we believe that the alignment of the magnetic cloud axis should be approximately related to its boundary normal directions,

Table 2. Summary of Longitudes and Latitudes of "Boundary" Normals in Comparison to the Magnetic Cloud Axis

Boundary Name	Longitude*	Latitude*
Upstream shock normal	192°	-36°
Cloud's front boundary (TD) normal	184°	-3°
Magnetic cloud axis - 90° longitude	201°	-12°
Internal "shock" normal + 90° longitude	218°	25°
Downstream interface normal	194°	37°

*Longitudes and latitudes in GSE coordinates

determined locally, if the simple model of a cylindrical surface for the cloud is at all realistic, as we believe it is for this event, at least in the ecliptic plane, given that the cloud's axis is nearly in the ecliptic plane. That is, these boundary normals should be approximately perpendicular to the magnetic cloud's axis, and this is what Table 2 and Figure 10 show, to a surprisingly good approximation: Figure 10 shows near alignment of the normals at points A(upstream shock), B(front TD), and D(downstream TD in the interface region characterized typically by the normal from Figure 6), where the longitudes (based on 0° meaning "toward" the Sun, as usual) are 192°, 184°, and 194°, respectively. As Table 2 emphasizes, these are all close to the quantity (90° + cloud axis) = 201°. We believe that these values justify our assumptions of the applicability of a (simple) cylindrical magnetic cloud model and that the model-cloud axis should provide a good longitudinal estimator for the local boundaries, front and back, and finally that the cloud was the driver for the upstream shock.

The normal we obtain for the internal shock-like structure, assuming that it is a shock and that our shock-applied analysis has legitimacy, has an unusual direction (longitude of 111°). If the normal is to be consistent with a co-rotating shock, it would normally be expected to be around 194°, i.e., aligned with the interface normal at point D. The approximately 90° difference from the nearly radial direction would be hard to explain if the internal "shock" pulse is a result of the stream interaction with the magnetic cloud. The pulse's surface is obviously not travelling like the forward shock driven by the cloud but seems to be traveling nearly along the axis of the magnetic cloud (flux rope), at least at Wind's moment of observation. Perhaps it can be viewed as an MHD pulse (at the Sun) propagating with its normal tending to be aligned along the magnetic cloud axis at this particular sighting position. The propagation speed for the segments of this "shock," along its surface, will depend on what plasma conditions it experiences upstream, and this region consists mainly of the strong magnetic fields of the magnetic cloud, etc., which may, to some extent, effect the shock's propagation and distort its original surface shape. Any asymmetrical (but unknown) birth conditions would further cause surface distortion.

The picture summarized by Figure 10 is the result of five separate and independent quantitative boundary analyses, which depended on independent sets of data in relatively small analysis intervals, except for the cloud model analysis which depended on a large (≈ 30 hours) interval. There is striking consistency.

5. Summary

We presented an analysis of the Wind observations of a magnetic cloud, its boundaries, and surrounding structures that occurred during October 18 - 21, 1995. The magnetic field lines in the magnetic cloud were shown to have a helical geometry, as one expects for an approximately force-free flux rope. The magnetic cloud, whose diameter was about 1/4 AU, had an axis only about 20° from perpendicular to the Sun-Earth line, and it was nearly in the ecliptic plane, not an uncommon attitude for interplanetary magnetic clouds at 1 AU at low heliospheric latitudes. The magnetic field strength profile differed from the prediction of a static constant-alpha model, possibly both because the magnetic cloud was "old" and no longer expanding at 1 AU and because of its interaction with a corotating stream which was overtaking it. A shock was observed ahead of the magnetic cloud, presumably generated by the differential motion of the magnetic cloud with respect to the upstream medium. A second shock-like pulse was observed inside the magnetic cloud, near its rear boundary, and analyzed to be locally propagating nearly along the axis of the cloud. One possibility for this shock-like pulse was that it was driven by the corotating stream that was interacting with the rear of the magnetic cloud, but the direction of propagation seems hard to reconcile with that proposition. Another possibility is that the shock's origin was associated with interplanetary ejecta originating at the Sun, and then propagating in a nonspherical front partly caused by the irregular solar wind in and around the magnetic cloud (e.g., possibly by refraction and/or reflection) and partly by its birth conditions, which are now not known. Much is inconclusive about the nature of this abrupt feature. The interaction region between the magnetic cloud and the corotating stream was complex. There may have been two stream interfaces, one possibly at the rear boundary of the magnetic cloud and a second several hours later. In the post-cloud region prominent Alfven waves were seen occurring for about 2 days, October 20 and 21. As complex as the history of these events must have been (especially at the Sun), at the time of Wind observations the estimated attitudes of the relevant structure boundaries, as summarized in Figure 10, appear to provide a surprisingly coherent and consistent superstructure with only the internal shock-like pulse providing a mystery, although the physical nature of the cloud-stream interface is also not yet completely understood.

The observations discussed above suggest many further studies [see, e.g., *Burlaga et al.* 1996], some of which are being carried out presently. One class of studies concerns further detailed observations from the Wind spacecraft, which we only touched upon in discussing the internal shock. For example, what is this structure's origin and why does it have such an unexpected surface normal? And what is the nature of the clearly monotonic and prolonged downstream waves at this shock? A second class of studies concerns further relations between the observations of Wind and Geotail, which was also in the solar wind for part of this time; these should provide new insights into the structure of the magnetic cloud, boundaries, filaments, small-scale structures, turbulence, etc. Perhaps the most important class of studies concerns the detailed connection to the solar origin of the magnetic cloud; see, for example, the recent work of *Smith*

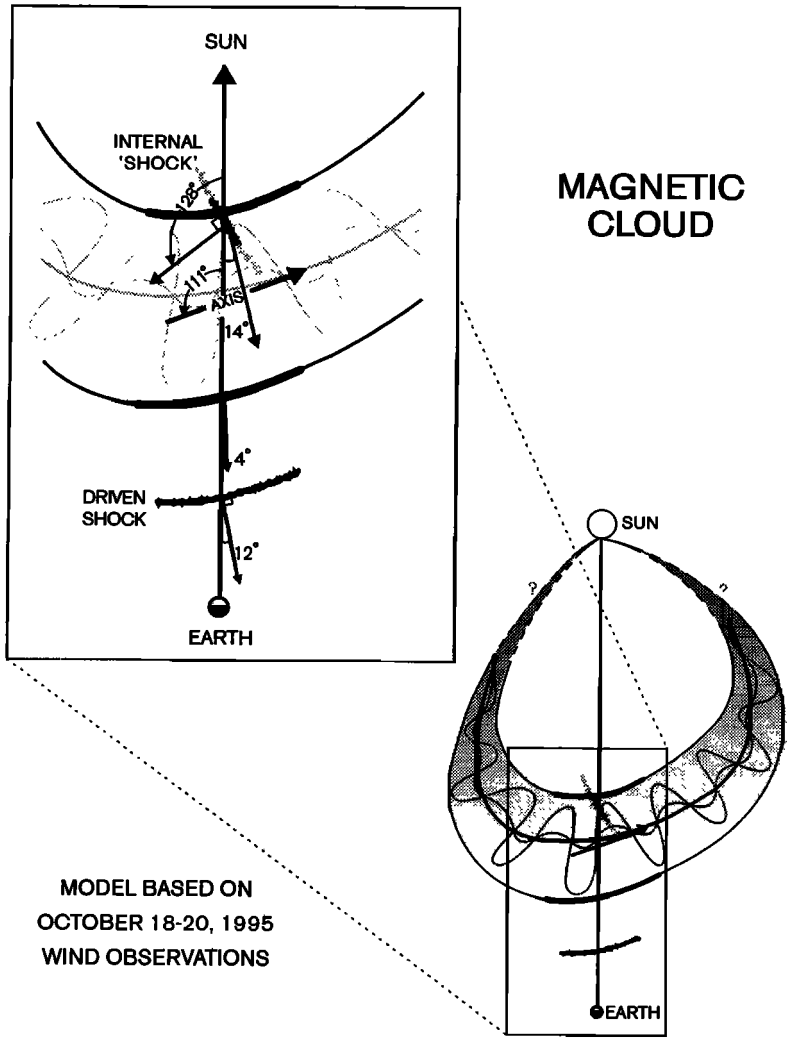

Figure 10. A summary sketch of the ecliptic plane cross-section of the magnetic cloud, stressing its longitudinal attitude with respect to its boundaries and (especially in the blown-up view) in comparison to the impinging shock-like pulse internal to the cloud and to the upstream shock wave. The global view is shown to put the observed portion (that along the Sun-Earth line through the cloud) in context, as interpreted earlier by *Burlaga et al.* [1990], but as the question marks show, we are not implying any direct knowledge about its solar origin in this study. Note that both views are presented approximately to scale along the radial line from the Sun. All surface normal vectors are direction indicators and strictly represent unit normals, regardless of lengths shown; variable lengths were done for clarity.

et al. [1997], who suggest a possible solar source for this series of interplanetary events. Also important, of course, is the magnetic cloud's interaction with the Earth and its consequences, specifically its influence on the magnetosphere, ionosphere, and thermosphere, concerning which we briefly discussed and displayed some specific time profiles of expected interplanetary triggers (the VB_S and ϵ parameters) in comparison to the *Kp* index.

A primary motivation for this report was to provide some preliminary, basic information on the solar wind properties and related analyses of this series of events needed for the above studies and other studies related to this magnetic cloud and stream interface.

Acknowledgments. M. Acuna, the ISTP Project Scientist, deserves special thanks for his role in this complex project. The arrival of the event which we have identified as a magnetic cloud was communicated to one of us (W.H.M.) in near real time by R. Zwickl at NOAA/ERL. We thank J. Jones for running the fitting program for the magnetic cloud, D. Berdichevsky for special data handling, M. Peredo for helpful comments on the manuscript, D. Fairfield and S. Kokubun or providing information on a feature in the Geotail magnetic field data, and Jennifer Matthews for some very nice art work. The work at MIT was supported in part by NASA GSFC under grant NAG 5-2839, and the work at UNH was supported by NASA under grant NAG 5-2834. Finally, we thank a referee for helpful comments on the Alfven wave portion and on the *Kp* index.

The Editor thanks K. Marubashi and another referee for their assistance in evaluating this paper.

References

Abraham-Shrauner, B., and S. H. Yun, Interplanetary shocks seen by Ames plasma probe on Pioneer 6 and 7, *J. Geophys. Res.*, *81*, 2097, 1976.

Akasofu, S.-I., Energy coupling between the solar wind and the magnetosphere, *Space Sci. Rev.*, *28*, 121, 1981.

Baker, D. N., S.-I. Akasofu, W. Baumjohann, J. W. Bieber, D. H. Fairfield, E. W. Hones Jr., B. Mauk, R. L. McPherron, and T. E. Moore, Substorms in the magnetosphere, *Solar Terrestrial Physics: Present and Future, NASA ref. publ.* 1120, 8-1, 1984.

Behannon, K. W., L. F. Burlaga., and A. Hewish, Structure and evolution of compound streams at 1 AU, *J. Geophys. Res., 96*, 21,213, 1991.

Burlaga, L. F., Magnetic clouds: Constant alpha force-free configurations, *J. Geophys. Res., 93*, 7217, 1988.

Burlaga, L. F., Magnetic clouds, in *Physics of the Inner Heliosphere*, vol. 2, edited by R. Schwenn and E. Marsch, p. 1, Springer-Verlag, New York, 1991.

Burlaga, L. F., *Interplanetary Magnetohydrodynamics*, Oxford Univ. Press, New York, 1995.

Burlaga, L. F., E. Sittler, F. Mariani, and R. Schwenn, Magnetic loop behind an interplanetary shock: Voyager, Helios and IMP-8 observations, *J. Geophys. Res., 86*, 6673, 1981.

Burlaga, L. F., R. Lepping, and J. Jones, Global configuration of a magnetic cloud, *Physics of Flux Ropes, Geophys. Monogr. Ser.*, vol. 58, edited by C. T. Russell, E. R. Priest and L. C. Lee, p. 373, AGU, Washington D. C., 1990.

Burlaga, L. F., R. P. Lepping, W. H. Mish, K. W. Ogilvie, A. Szabo, A. J. Lazarus, and J. T. Steinberg, A magnetic cloud observed by WIND on October 18 - 20, 1995, internal document, NASA, Goddard Space Flight Cent., Lab. for Extraterrestrial Phys., Feb., 1996.

Chen, J. A., S. Slinker, J. A. Fedder, and J. G. Lyon, Simulation of geomagnetic storms during the passage of magnetic clouds, *Geophys. Res. Lett., 22*, 1794, 1995.

Choe, J. T., D. B. Beard, and E. C. Sullivan, Precise calculation of the magnetosphere surface for a tilted dipole, *Planet. Space Sci., 21*, 485, 1973.

Fairfield, D. H., Average and unusual locations of the Earth's magnetopause and bow shock, *J. Geophys. Res., 76*, 6700, 1971.

Farrugia, C. J., and L. F. Burlaga, A fast-moving magnetic cloud and features of its interaction with the dayside magnetosheath, in *The Solar Wind-Magnetosphere System*, edited by S. Bauer and H. K. Biernat, p. 33, Austrian Acad. of Sci. Press, Vienna, 1994.

Farrugia, C. J., M. P. Freeman, S. W. H. Cowley, D. J. Southwood, M. Lockwood, and A. Etemadi, Pressure-driven magnetopause motions and attendant response on the ground, *Planet. Space Sci.*, 37, 589, 1989.

Farrugia, C. J., L. F. Burlaga, P. Freeman, R. P. Lepping, and V. Osherovich, A comparative study of expanding force-free constant alpha magnetic configurations with application to magnetic clouds, in *Solar Wind Seven*, edited by R. Schwenn, p. 61, Pergamon, New York, 1992.

Farrugia, C. J., L. F. Burlaga, V. Osherovich, I. G. Richardson, M. P. Freeman, R. P. Lepping, and A. Lazarus, A study of an expanding interplanetary magnetic cloud and its interaction with the Earth's magnetosphere: The interplanetary aspect, *J. Geophys. Res., 98*, 7621, 1993a.

Farrugia, C. J., M. P. Freeman, L. F. Burlaga, R. P. Lepping, and K. Takahashi, The Earth's response under continued forcing; Substorm activity during the passage of an interplanetary magnetic cloud, *J. Geophys. Res., 98*, 7657, 1993b.

Farrugia, C. J., I. G. Richardson, L. F. Burlaga, R. P. Lepping, and V. A. Osherovich, Simultaneous observations of solar MeV particles in a magnetic cloud and in the Earth's northern tail lobe: Implications for the global field line topology of magnetic clouds, and for the entry of solar particles into the magnetosphere during cloud passage, *J. Geophys. Res., 98*, 15,497, 1993c.

Farrugia, C. J., R. J. Fitzenreiter, L. F. Burlaga, N. V. Erkaev, V. A. Osherovich, H. K. Biernat, and A. Fazakerley, Observations in the sheath region ahead of magnetic clouds and in the dayside magnetosheath during cloud passage, *Adv. Space Res., 14*(7), 105, 1994.

Farrugia, C. J., N. V. Erkaev, H. K. Biernat, and L. F. Burlaga, Anomalous magnetosheath properties during Earth passage of an interplanetary magnetic cloud, *J. Geophys. Res., 100*, 19,245, 1995a.

Farrugia, C. J., L. F. Burlaga, and V. A. Osherovich, The magnetic flux rope versus the spheromak as models for interplanetary magnetic clouds, *J. Geophys. Res., 100*, 12,293, 1995b.

Farrugia, C. J., R. P. Lepping, L. F. Burlaga, A. Szabo, D. Vassiliadis, P. Stauning, and M. P. Freeman, The WIND magnetic cloud of October 18-20, 1995: Implications for the magnetosphere, *EoS Trans.* AGU, 77(17), Spring Meet. Suppl., S241, 1996.

Farrugia, C. J., L. F. Burlaga, and R. P. Lepping, Magnetic clouds and the quiet-storm effect at Earth, in *Geophys. Monogr. Series*, edited by B. T. Tsurutani et al., AGU, Washington, D. C., 1997.

Freeman, M. P., C. J. Farrugia, L. F. Burlaga, M. R. Hairston, M. Greenspan, J. M. Ruohoniemi, and R. P. Lepping, The interaction of a magnetic cloud with the Earth: Ionospheric convection in the northern and southern hemispheres for a wide range of quasi-steady interplanetary magnetic field conditions, *J. Geophys Res., 98*, 7633, 1993.

Gonzalez, W. D., B. T. Tsurutani, A. L. C. Gonzalez, E. J. Smith, F. Tang, and S.-I. Akasofu, Solar wind magnetosphere coupling during intense magnetic storms (1978 - 1979), *J. Geophys. Res., 94*, 8835, 1989.

Goodrich, C. C., Numerical simulations of quasi-perpendicular collisionless shocks, *Collisionless Shocks in the Heliosphere: Reviews of Current Research, Geophys. Monogr. Ser.*, vol. 35, edited by B. T. Tsurutani and R. G. Stone, p. 153, AGU, Washington, D. C., 1985.

Goldstein, H., On the field configuration in magnetic clouds, in *Solar Wind Five*, edited by M. Neugebauer, *NASA Conf. Publ.*, 2280, 731, 1983.

Gosling, J. T., Coronal mass ejections and magnetic flux ropes in interplanetary space, in *Physics of Magnetic Flux Ropes, Geophys. Monogr. Ser.*, vol. 58, edited by C. T. Russell, E. R. Priest, and L. C. Lee, p. 343, AGU, Washington, D. C., 1990.

Hundhausen, A. J., The solar wind, in *Introduction to Space Physics*, edited by M. G. Kivelson and C. T. Russell, 91, Cambridge Univ. Press, New York, 1995.

Klein, L. W., and L. F. Burlaga, Interplanetary magnetic clouds at 1 AU, *J. Geophys. Res., 87*, 613, 1982.

Knipp, D. J., et al., Ionospheric convection response to slow, strong variations in a northward interplanetary magnetic field: A case study for January 14, 1988, *J. Geophys. Res.*, 98, 19,273, 1993.

Kumar, A., and D. M. Rust, Interplanetary magnetic clouds, helicity conservation, and current-core flux-ropes, *J. Geophys. Res., 101*, 15,667, 1996.

Lepping, R. P., and L. F. Burlaga, Geomagnetopause surface fluctuations observed by Voyager-1, *J. Geophys. Res., 84*, 7099, 1979.

Lepping, R. P., J. A. Jones, and L. F. Burlaga, Magnetic field structure of interplanetary magnetic clouds at 1 AU, *J. Geophys. Res., 95*, 11,957, 1990.

Lepping, R. P., L. F. Burlaga, B. T. Tsurutani, K. W. Ogilvie, A. J. Lazarus, D. S. Evans, and L. W. Klein, The interaction of a very large interplanetary magnetic cloud with the magnetosphere and with cosmic rays, *J. Geophys. Res., 96*, 9425, 1991.

Lepping, R. P., et al., The WIND magnetic field investigation, The Global Geospace Mission, *Space Sci. Rev. 71*, 207, 1995.

Lepping, R. P., A. Szabo, K. W. Ogilvie, R. J. Fitzenreiter, A. J. Lazarus, and J. T. Steinberg, Magnetic cloud-bow shock interaction: WIND and IMP-8 observations, *Geophys. Res. Lett.*, 23, 1195, 1996.

Leroy, M. M., D. Winske, C. C. Goodrich, C. S. Wu, and K. Papadopoulos, The structure of perpendicular bow shocks, *J. Geophys. Res., 87*, 5081, 1982.

Lundquist, S., Magnetohydrostatic fields, *Ark. Fys., 2*, 361, 1950.

Marubashi, K., Structure of the interplanetary magnetic clouds and their solar origins, *Adv. Space Res., 6*(6), 335, 1986.

Mish, W. H., J. L. Green, M. G. Reph, and M. Peredo, ISTP Science data systems and products, *Space Sci Rev., 71*, 815, 1995.

Newbury, J. A., and C. T. Russell, Observations of a very thin collisionless shock, *Geophys. Res. Lett., 23*, 781, 1996.

Ogilvie, K. W., et al., SWE, A comprehensive plasma instrument for the WIND spacecraft, The Global Geospace Mission, *Space Sci. Rev., 71*, 55, 1995.

Osherovich, V. A., C. J. Farrugia, and L. F. Burlaga, Nonlinear evolution of magnetic flux ropes, 1, The low-beta limit, *J. Geophys. Res., 98*, 13,225 1993a.

Osherovich, V. I., C. J. Farrugia, and L. F. Burlaga, Dynamics of aging magnetic clouds, *Adv. Space Res., 13*(6), 57, 1993b.

Osherovich, V. A., C. J. Farrugia, and L. F. Burlaga, The non-linear evolution of magnetic flux ropes, 2, Finite beta plasma, *J. Geophys. Res., 100*, 12,307, 1995.

Perreault P., and S.-I. Akasofu, A study of geomagnetic storms, *Geophys. J. R. Astron. Soc., 54*, 547, 1978.

Rust, D. M., Spawning and shedding of helical magnetic fields in the heliosphere, *Geophys. Res. Lett., 21*, 241, 1994.

Smith, Z., S. Watari, M. Dryer, P. K. Manoharan, and P. S. McIntosh, Identification of the solar source for the 18 October 1995 magnetic cloud, *Sol. Phys.*, in press, 1997.

Song, P., R. C. Elphic, and C. T. Russell, ISEE 1 & 2 observations of the oscillating magnetopause, *Geophys. Res. Lett.*,15, 744, 1988.

Southwood, D. J., and M. G. Kivelson, The magnetohydrodynamic response of the magnetospheric cavity to changes in solar wind pressure, *J. Geophys. Res., 95*, 2301, 1990.

Tsurutani, B. T., and W. D. Gonzalez, The cause of high intensity long-duration continuous AE activity (HILDCAAs): Interplanetary Alfven wave trains, *Planet. Space Sci.*, 35, 405, 1987.

Tsurutani, B. T. and W. D. Gonzalez, The interplanetary causes of magnetic storms: A review, *in Geophysical Monograph Series*, edited by B. T. Tsurutani et al., AGU, Washington, D. C., 1997.

Tsurutani, B. T., W. D. Gonzalez, F. Tang, S.-I. Akasofu, and E. J. Smith, Origin of interplanetary southward magnetic field responsible for major magnetic storms near solar maximum (1978-1989), *J. Geophys. Res., 93*, 8519, 1988.

Tsurutani, B. T., C. M. Ho, J. K. Arballo, B. E. Goldstein, and A. Balogh, Large amplitude IMF fluctuations in corotating interaction regions: Ulysses at midlatitudes, *Geophys. Res. Lett.*, 22, 3397, 1995a.

Tsurutani. B. T., et al., Interplanetary origin of geomagnetic activity in the declining phase of the solar cycle, *J. Geophys. Res., 100*, 21,717, 1995b.

Vandas, M. S., M. F. Fisher, M. Dryer, Z. Smith, and T. Detman, Simulation of magnetic cloud propagation in the inner heliosphere in two-dimensions 1. A loop perpendicular to the ecliptic plane, *J. Geophys. Res., 100*, 12,285, 1995.

Vandas, M. S., M. F. Fisher, M. Dryer, Z. Smith, and T. Detman, Simulations of magnetic cloud propagation in the inner heliosphere in 2 dimensions, 2, A loop parallel to the ecliptic plane and the role of helicity, *J. Geophys. Res., 101*, 2505, 1996.

Wilson, R. M., and E. Hildner, Are interplanetary magnetic clouds manifestations of coronal transients at 1 AU?, *Sol. Phys., 91*, 169, 1984.

Wilson, R. M., and E. Hildner, On the association of magnetic clouds with disappearing filaments, *J. Geophys. Res., 91*, 5867, 1986.

L. F. Burlaga, R. P. Lepping, W. H. Mish, K. W. Ogilvie, A. Szabo, and D. Vassiliadis, Laboratory for Extraterrestrial Physics, NASA Goddard Space Flight Center, Geenbelt, MD 20771. (e-mail: rpl@leprpl.gsfc.nasa.gov)

C. J. Farrugia and L. Janoo, Department of the Study of Earth, Oceans, and Space, University of New Hampshire, Durham, NH 03824.

A. J. Lazarus and J. T. Steinberg, Center for Space Research, Massachusetts Institute of Technology, Cambridge, MA 02139.

F. Mariani, Dipartimento di Fisica, Universita Tor Vergata, Roma 00173, Italy.

(Received August 26, 1996; revised December 6, 1996;
accepted January 13, 1997.)